Stability Charts for Simple Earth Slopes allowing for Tension Cracks

B. F. COUSINS
Senior Lecturer in Civil Engineering, University of Tasmania

SUMMARY In a previous paper by the author (Cousins, 1978) stability charts were presented for simple earth slopes ignoring tension cracks. Tension cracks are usually the first sign of impending failure in cohesive soils and therefore should be taken into account. In this paper the effect of tension cracks both dry and filled with water is investigated. Stability charts are presented for toe circles with no water in the tension crack and for a homogeneous pore pressure ratio r_u = 0, 0.25 and 0.5. A chart is also given for pore pressure ratio r_u = 0 with the tension crack filled with water. The charts have been constructed assuming the worst possible location and depth of the tension crack. As such they represent a lower bound for the safety factor. The maximum reduction in safety factor of 40% was found for slope angle $\alpha = 60^o$ and dimensionless parameter $\lambda_{c\phi} = 20$ with the tension crack filled with water. For most cases the reduction was much less than this.

1 INTRODUCTION

Most charts for investigating the stability of simple homogeneous slopes do not allow for tension cracks. See, for example, Bishop and Morgenstern (1960), Spencer (1967), Janbu (1967) and Cousins (1978). One exception is Hoek and Bray's (1977) charts. Hoek and Bray locate the tension crack so that the safety factor for the slope is a minimum for the slope geometry and groundwater conditions considered. The charts do not give the depth of tension crack used. Also their method for dealing with pore pressure is different from most other charts. In this paper pore pressure will be taken into account by assuming a homogeneous pore pressure ratio, r_u.

There is much conjecture on what value to take for the tensile crack depth in cohesive soils (Chowdhury 1978). An expression often used is

$$z_c = \frac{2c}{\gamma} \tan\left(\frac{\pi}{4} + \frac{\phi}{2}\right) \qquad (1)$$

where c and ϕ apply to total stresses. In any case this type of expression cannot conveniently be used in a non-dimensional treatment of slope stability.

A better approach is to assume that the tension crack depth and location are chosen to give the lowest possible safety factor. In this paper the tension crack depth is made non dimensional by dividing by the height of the slope. The depth of the tension crack has been limited to half the height of the slope as suggested by Terzaghi (1943).

Slope failure often occurs during heavy rainfalls. This suggests that tension cracks if present may become partially filled with water which acts as a trigger to failure. The efeect of water in tension cracks is allowed for in this paper by assuming that the tension crack is filled with water having a unit weight equal to half that of the bulk unit weight of the soil. This assumption is necessary to make the effect non dimensional.

In the past it has been suggested (Terzaghi, 1943) that the effect of tension cracks can be allowed for by reducing the cohesive strength. This paper will eliminate the need for such assumptions.

2 NOTATION

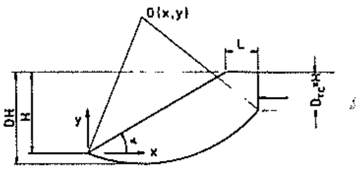

Figure 1 Notation for simple slope

- c' = cohesion strength based on effective stresses
- c'_m = mobilized cohesion stress
- D = depth factor
- D_{TC} = tension crack depth factor
- F = factor of safety
- H = height of slope
- L = distance from crest of slope to tension crack
- N_F = $F\gamma H/c'$ = $\gamma H/c'_m$ = stability number
- r_u = pore pressure ratio
- α = slope angle in degrees
- γ = bulk unit weight of soil
- $\lambda_{c\phi}$ = $\gamma H \tan\phi'/c'$ = dimensionless parameter
- ϕ' = internal friction angle based on effective stresses
- ϕ'_m = mobilized friction angle.

3 LIMIT EQUILIBRIUM METHOD USED

The method of analysis used in this investigation is simply an extension of the method used in a previous paper (Cousins 1978). The pattern search method of optimization (Adley and Dempster, 1974) is used to find the minimum value for the stability number, N_F for a given slope angle α, pore pressure ratio r_u, and mobilized friction angle ϕ'_m. Figure 2 gives a simplified flow chart of how the stability number N_F is determined for a given value of the dimensionless parameter, $\lambda_{c\phi}$. However, the pattern search method did not always work for reasons discussed later.

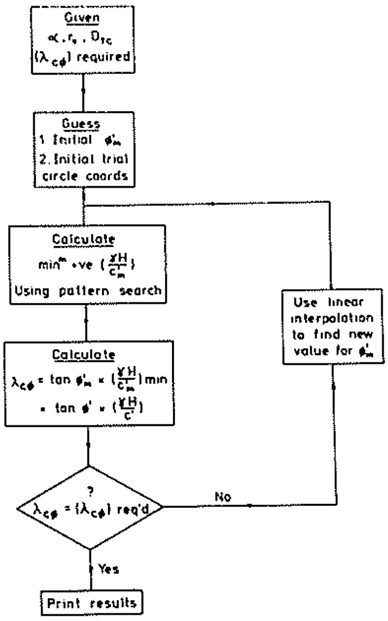

Figure 2 Flow chart for determination of stability number N_F

4 LOCATION OF TENSION CRACK

Trial slip circles are defined in this investigation by fixing circle centres and specifying a depth factor D or a common point. The location of a tension crack of a given depth is then automatically fixed. It is located at the highest point on the slope where the height between the ground surface and the failure arc is equal to the required tension crack depth. See Figure 1. It is possible for the height between the ground surface and the failure arc to be less than the required tension crack depth along the whole length of the arc. In this case the trial circle is not allowed.

The computer program allows the tension crack to progress down the slope face if this is geometrically possible. However, it is not possible in a homogeneous soil with a uniform pore pressure ratio distribution for the exit point of the critical circle to progress down the slope face. This applies whether the tension crack is filled with water or not. The reason for this is quite simple. Suppose the tension crack for the critical circle is located on the slope face. The height of the slope could then be increased indefinitely without altering the critical circle since the forces acting on the critical circle mass would be unchanged. Clearly the supposition is unrealistic. This is verified in all cases by the computer results.

5 OPTIMIZATION PROBLEMS

A typical contour map for N_F is given in Figure 3. It shows the critical circle with its tension crack on the crest of the slope. It also illustrates one of the problems of the investigation. The location of the centre of the critical circle is close to the non permissible boundary. In fact for higher values of slope angle α and $\lambda_{c\phi}$ the centre of the critical circle lies on the non permissible boundary.

6 VARIATION OF STABILITY NUMBER WITH TENSION CRACK DEPTH

Plots of normalized stability number N_F against tension crack depth factor for toe circles are given in Figures 4 and 5 for slope angles of 20^o and 45^o and a range of $\lambda_{c\phi}$ values.

For the case of no water in the tension crack all the curves show an initial decrease in the stability number N_F followed by an increase. Clearly the ϕ = 0 value gives the greatest reduction in stability number for both slope angles, the extent of the reduction increasing as the slope angle increases. The maximum reduction of 14% occurs when the slope angle $\alpha = 60^o$ and $\phi = 0$. It must be remembered that these results apply to toe circles. A reduction of 10% occurs for the depth factor D = 1 case for $\alpha = 20^o$. For $\alpha = 45^o$ the toe circles have a depth factor D almost equal to 1. The graphs clearly indicate that a particular tension crack depth such as that given by equation (1) will give a stability number higher or lower than the no tension crack case depending on the relative values of the parameters involved.

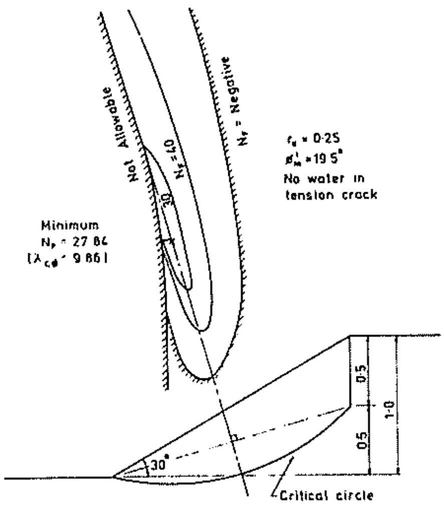

Figure 3 Typical contour map for stability number N_F

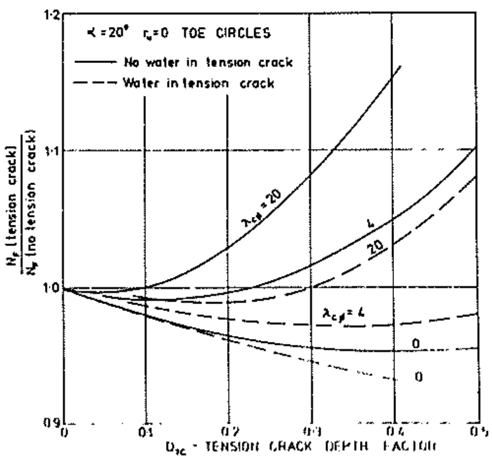

Figure 4 Variation of stability number N_F with tension crack depth, $\alpha = 20^o$

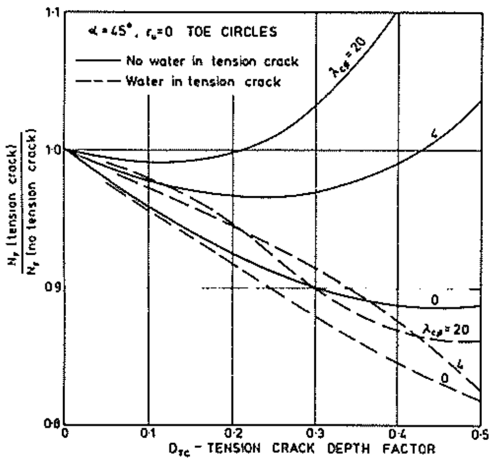

Figure 5 Variation of stability number N_F with tension crack depth, $\alpha = 45^o$

When the tension crack is filled with water the decrease in stability number N_F is higher than the no water case. The minimum also occurs at a higher tension crack depth factor. For the lower values of $\lambda_{c\phi}$ the stability number N_F is still decreasing at a tension crack depth factor D_{TC} equal to the cut off value of 0.5. The maximum reduction of 40% in stability number N_F occurs when the slope angle $\alpha = 60^o$.

7 STABILITY CHARTS FOR TOE CIRCLES

Clearly the number of charts would be too numerous if sets were given for a range of constant tension crack depth factors. It is more sensible to give charts based on a minimum stability factor N_F obtained by allowing the tension crack depth to vary. The program was modified to allow the tension crack depth factor corresponding to the minimum stability number to be determined. The required tension crack depth factor, D_{TC} was obtained to an accuracy of $\pm$ 0.01H.

Figures 6-8 give the minimum stability number N_F for the no water in the tension crack case for values of the pore pressure ratio = 0, 0.25 and 0.5 respectively. It should be noted that these charts have the same format as that given by Cousins, (1978). However, the slope angle α has been increased to a maximum of 60^o. This is possible because the presence of a tension crack eliminates the inter granular tension around the failure arc for the higher slope angles and pore pressure ratios. Even so the slope angle in Figure 8 has been limited to 50^o because of problems associated with the stress distribution around the failure arc. The concept of a pore pressure ratio is more relevant for the lower slope angles. For high slope angles and high values of $\lambda_{c\phi}$ the critical circle is quite superficial thus making it difficult to estimate a reasonable value for the average pore pressure ratio.

Curves are also given in Figures 6-8 which allow the critical tension crack depth factor D_{TC}, the toe circle depth factor D, and the mobilized friction angle ϕ'_m to be determined. In all cases examined the critical tension crack depth factor D_{TC} is greater than 0. However, the difference in stability number N_F is not significant for higher values of $\lambda_{c\phi}$ if the slope angle α is less than 20^o. The upper limit for D_{TC} of 0.5 is just reached when the slope angle equals 60^o.

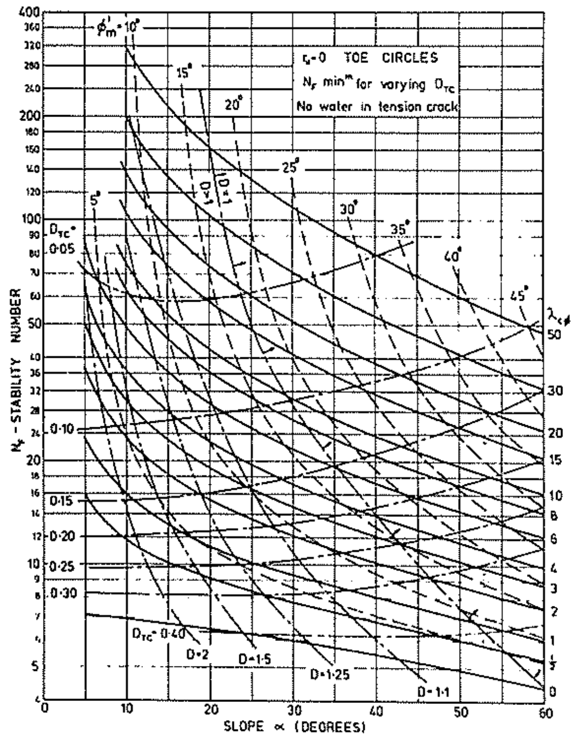

Figure 6 Stability number N_F for no water in tension crack, $r_u = 0$

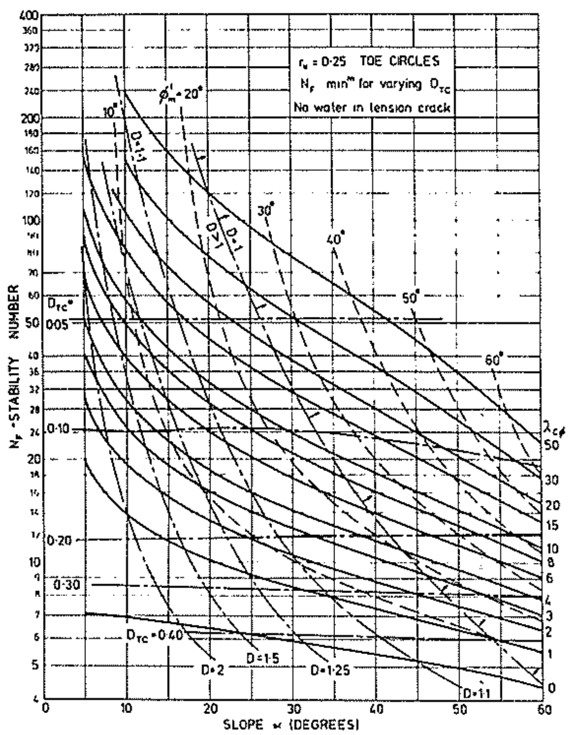

Figure 7 Stability number N_F for no water in tension crack, $r_u = 0.25$

Figure 9 gives the stability chart for $r_u = 0$ when the tension crack is filled with water. In this case the upper limit for D_{TC} of 0.5 is reached at low values of slope angle, α. A comparison with Figure 6 indicates that the importance of water in the tension crack increases with slope angle, α.

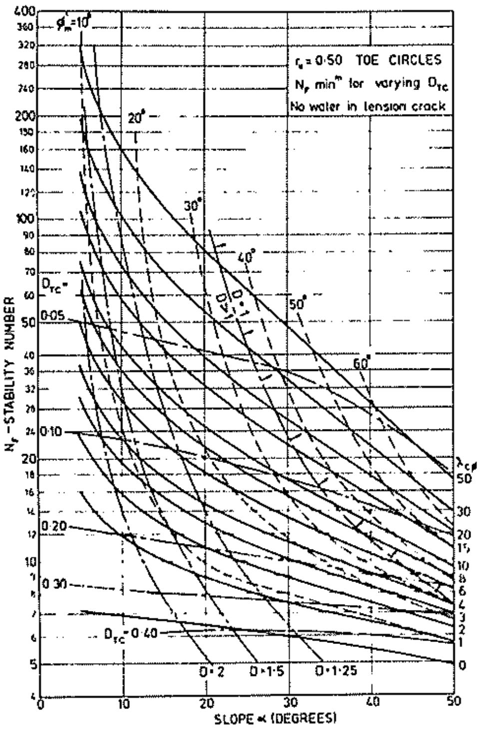

Figure 8 Stability number N_F for no water in tension crack, $r_u = 0.5$

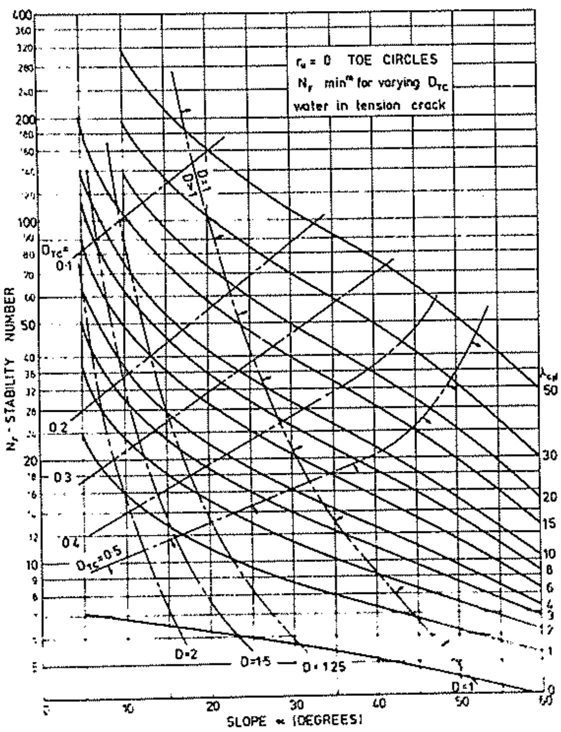

Figure 9 Stability number N_F for water in tension crack, $r_u = 0$

The location of the critical tension crack is given in Figures 10 and 11 for the no water in the tension crack case and the water in the tension crack case respectively. In Figure 10 the exit point of the critical circle for the no tension crack case is also given to aid comparison. Allowing for tension cracks causes the exit point on the crest of the slope to move closer to the slope face as expected. For higher values of slope angle the critical tension crack is located approximately half way between the crest point and the exit point for the no tension crack case. Figure 11 indicates that the critical tension crack moves even closer to the crest if the tension crack is filled with water. For slope angles $\alpha > 25^o$ and $\lambda_{c\phi} > 3$ the critical tension crack is actually located at the crest.

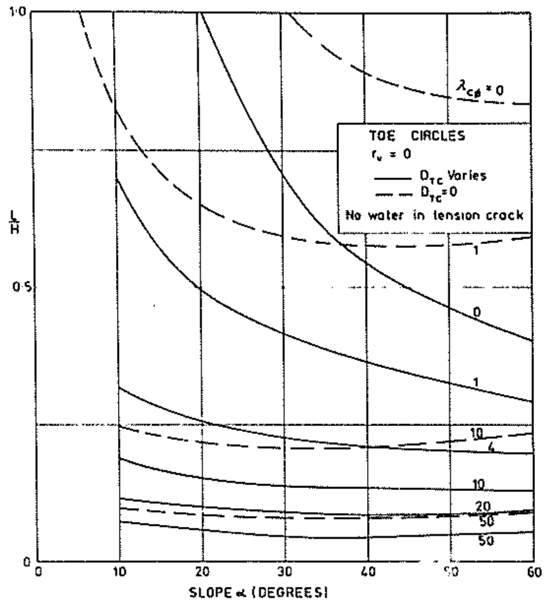

Figure 10 Values of L/H for no water in tension crack

8 EXAMPLE

Find the safety factor with and without allowing for tension cracks for a simple slope. The relevant parameters are: H = 20m; γ = 20 kN/m^3; c' = 80 k Pa; ϕ' = 11.3^o; r_u = 0.
Thus $c'/\gamma H$ = 0.20 and $\lambda_{c\phi} = \gamma x H \tan\phi'/c'$ = 1.00.
No water in tension crack case:
Figure 6 gives N_F = 8.7, thus F = 8.7 x $c'/\gamma H$ = 1.74.
Also D = 1.09, D_{TC} = 0.29.
Water in tension crack case:
Figure 9 gives N_F = 7.9, thus F = 1.58.
In this case D = 1.1, D_{TC} = 0.50.
No tension crack case:
The author's previous charts (Cousins, 1978) gives N_F = 9.15, thus F = 1.83 and D = 1.09.
For this example allowing for the worst possible condition gives a reduction of 14% in the safety factor over the no tension crack case.

9 CONCLUSIONS

1 Assuming the most severe combination of location and depth of tension crack gives a maximum reduction of 20% over the no tension crack case for values of slope angle less than 45^o.

2 The stability number N_F for a particular tension

crack depth may be higher or lower than for the no tension crack case. However, the minimum stability number is always reduced if the tension crack depth is allowed to vary.

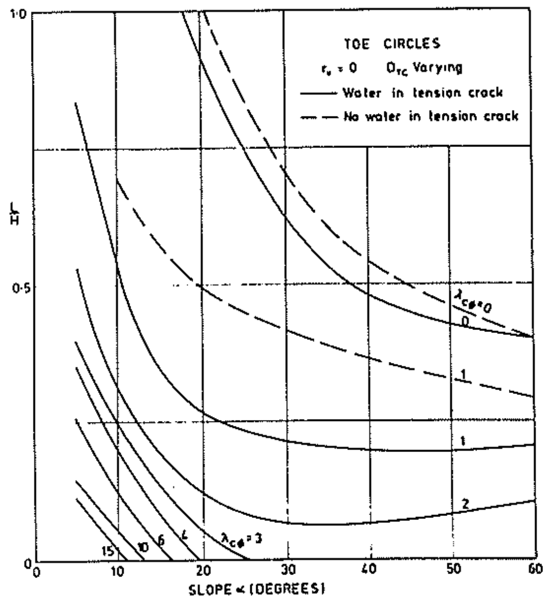

Figure 11 Values of L/H for water in tension crack

3 The location of the critical tension crack is quite close to the crest of the slope for the no water in the tension crack case and even closer if the tension crack is filled with water. For slope angles $\alpha > 25^{\circ}$ and $\lambda_{c\phi} > 3$ the critical tension crack is located at the crest if the crack is filled with water.

4 The restrictions placed on Janbu's (1967) method for allowing for the pore pressure ratio given in a previous paper (Cousins 1978) are still applicable when tension cracks are allowed for.

10 REFERENCES

ADLEY, P.R. and DEMPSTER, M.A.H. (1974). Introduction to optimization Methods. London, Chapman and Hall.

BISHOP, A.W. and MORGENSTERN, N.R. (1960). Stability Coefficients for Earth Slopes. Geotechnique, Vol. 10, No. 4, pp 129-147.

CHOWDHURY, R.N. (1978). Slope Analysis. Amsterdam, Elsevier Scientific Publishing Company.

COUSINS, B.F. (1978). Stability Charts for Simple Earth Slopes. Journal of the Geotechnical Engineering Division, ASCE Vol 104, No. GT2, Proc. Paper 13572.

HOEK, E. and BRAY, J.W. (1977). Rock Slope Engineering. London, Institution of Mining and Metallurgy.

JANBU, N. (1967). Discussion of Paper - Dimension-less Parameters for Homogeneous Earth Slopes by Bell, J.M., Journal of the Soil Mechanics and Foundations Division, ASCE. Vol. 93, No. SM6. pp 367-374.

SPENCER, E. (1967). A Method of Analysis of the Stability of Embankments Assuming parallel Inter-Slice Forces. Geotechnique, Vol. 17, No. 1, pp. 11-26.

TERZAGHI, K. (1943). Theoretical Soil Mechanics. New York, McGraw Hill.